

KIPT 2008-3

National Academy of Sciences of Ukraine
National Science Center
«Kharkov Institute of Physics and Technology»



**MATHEMATICAL SIMULATION OF GAMMA-RADIATION
ANGLE DISTRIBUTION MEASUREMENTS**

Preprint

Kharkov
2008

MATHEMATICAL SIMULATION OF GAMMA-RADIATION ANGLE DISTRIBUTION MEASUREMENTS: Preprint 2008-3 / V.G. Batiy, Ye.V. Batiy, V.V. Yegorov, D.V. Fedorchenko, O.A. Kaftanatina, M.A. Khazhmuradov, N.A. Kochnev, V.V. Selyukova, A.I. Stojanov, S.I. Prohoretz, I.M. Prohoretz, Ye.V. Rudychev, V.P. Lukyanova. – Kharkov: NSC KIPT, 2008, - 19 p.

We developed mathematical model of the facility for gamma-radiation angle distribution measurement and calculated response functions for gamma-radiation intensities. We developed special software for experimental data processing, the "Shelter" object radiation spectra unfolding and Sphere detector (ShD) angle resolution estimation. Neuronet method using for detection of the radiation directions is given. We developed software based on the neuronet algorithm, that allows obtaining reliable distribution of gamma-sources that make impact on the facility detectors at the measurement point.

Fig. 15, Tab. 4, Ref.- 10 items.

МАТЕМАТИЧЕСКОЕ МОДЕЛИРОВАНИЕ ПРОЦЕССА ИЗМЕРЕНИЯ УГЛОВЫХ РАСПРЕДЕЛЕНИЙ ГАММА-ИЗЛУЧЕНИЯ: Препринт 2008-3/ В.Г. Батий, Е.В. Батий, В.В. Егоров, Д.В. Федорченко, О.А. Кафтанатина, М.А. Хажмуратов, Н.А. Кочнев, В.В. Селюкова, А.И. Стоянов, С.И. Прохорец, И.М. Прохорец, Е.В. Рудычев, В.П. Лукьянова. - Харьков: ННЦ ХФТИ, 2008, -19 с.

Разработана математическая модель многодетекторного блока установки для измерения углового распределения гамма-излучения и рассчитаны функции отклика интенсивности гамма-излучения. Разработаны специальные вычислительные программы для обработки экспериментальных данных, восстановления спектра излучения объекта «Укрытие» и оценки углового разрешения шарового детектора (ШД). Приведена методика применения нейросетевой технологии для распознавания направления на множество источников излучения. На основе нейросетевого алгоритма разработана программа, позволяющая получить достоверное распределение гамма-источников, воздействующих на детекторы установки в точке измерения.

Рис. 15, табл. 4, список лит. – 10 назв.

INTRODUCTION

Work activities concerned with radiation hazard require effective personnel protection. Such work conditions appear during NPP operation, radwaste management, activities at Chornobyl NPP's "Shelter" object, radiation accident consequences elimination etc. Practical application of radiation shielding should be based on the information on the radiation sources locations and activities. The efficient device providing with such information is multidetector device ShD.

The main goal of this work was development of mathematical model of the facility for angular distribution measurements and mathematical simulation of measurement procedure.

1. Development of device mathematical model

ShD facility is the multidetector device in a shape of lead sphere with 32 uniformly placed collimating apertures (Fig. 1) [1-3]. Collimating aperture angle is 45° . At the bottom of collimating apertures cylinders with radiation detectors capsules are placed. Axis of the each cylinder coincides with sphere radius connecting sphere center with corresponding aperture center. 12 apertures belong to the inscribed icosahedrons corners and 20 – to the corresponding inscribed dodecahedron corners. Aperture centers angular coordinates are given in Table 1.

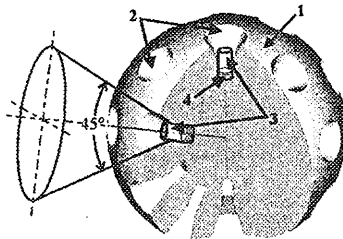


Fig. 1. Scheme of the ShD-1 for angular distribution measurement: 1 – lead solid; 2 – collimating apertures, 3 – capsules with detectors; 4 – CdZnTe-detectors

Further we shall consider the mathematical model for equivalent dose rate (EDR) angular distribution unfolding using experimental data [3].

Table 1. Coordinates of aperture centers

№	θ , degree	φ , degree	№	θ , degree	φ , degree
1	0	0	17	100,8	36
2	37,4	0	18	100,8	108
3	37,4	72	19	100,8	180
4	37,4	144	20	100,8	252
5	37,4	216	21	100,8	324
6	37,4	288	22	116,6	0
7	63,4	36	23	116,6	72
8	63,4	108	24	116,6	144
9	63,4	180	25	116,6	216
10	63,4	252	26	116,6	288
11	63,4	324	27	142,6	36
12	79,2	0	28	142,6	108
13	79,2	72	29	142,6	180
14	79,2	144	30	142,6	252
15	79,2	216	31	142,6	324
16	79,2	288	32	180	0

By definition, EDR angular distribution function $H(\theta, \varphi)$ is EDR due to radiation coming from the direction defined by θ and φ polar coordinates. Coordinate system origin coincides with ShD geometrical center. By definition, integral EDR at the ShD location is

$$H_{\text{int}} = \int_0^{2\pi} d\varphi \int_0^{\pi} d\theta \sin\theta H(\theta, \varphi). \quad (1)$$

Information about angular distribution is hold within recorded detector data. This allows approximate unfolding of EDR angular distribution function $H(\theta, \varphi)$.

ShD detectors register doze rate averaged over collimator's solid-angle. Solid angle value is determined by collimating apertures. Thus approximated distribution function equals to

$$H(\theta, \varphi) = \sum_{i=1}^{32} H_i \Theta(\theta, \varphi, \Omega_i), \quad (2)$$

where H_i – is EDR averaged over Ω_i solid angle; Ω_i – collimating aperture solid angle for i -th detector (see Table 1).

Function $\Theta(\theta, \varphi, \Omega_i)$ is defined as

$$\Theta(\theta, \varphi, \Omega) = \begin{cases} 1, & (\theta, \varphi) \in \Omega \\ 0, & (\theta, \varphi) \notin \Omega \end{cases}. \quad (3)$$

Thus, angular distribution function $H(\theta, \varphi)$ is defined by 32 \bar{H}_i parameters.

In general case EDR measured by detectors essentially depends on the ShD geometry and features. Each detector registers radiation passed not only directly through collimating aperture, but also that passed through ShD material. Thus, registered EDR value differs from given direction EDR by the value of this additional radiation. Complex device geometry precludes analytical calculation of the radiation passed through the ShD.

EDR for each detector can be expressed as

$$H_i^{\text{det}} = \bar{H}_i + \tilde{H}_i, \quad (4)$$

where \tilde{H}_i – additional EDR due to radiation passed through the detector unit material and registered by i -th detector; H_i^{det} – radiation dose rate registered by i -th detector.

\tilde{H}_i can be represented as

$$\tilde{H}_i = \sum_{\substack{j=1, \\ j \neq i}}^{32} \alpha_{ij} \bar{H}_j, \quad (5)$$

where α_{ij} – attenuation coefficients for radiation coming to Ω_j solid angle and registered by i -th detector. Coefficients α_{ij} can be found either from the ShD device geometry or by means mathematical simulation.

From relations (4) and (5) linear system for \bar{H}_i parameters follows defining radiation angular distribution function

$$\dot{H}_i + \sum_{\substack{j=1 \\ j \neq i}}^{32} \alpha_{ij} H_j = H_i^{\text{det}}. \quad (6)$$

Coefficients α_{ij} can be calculated using attenuation coefficients for ShD material. Usage of mathematical simulation methods is expedient for such calculations, in particular those based on Monte Carlo method, e.g., GEANT, PENELOPE and MCNP software.

Response functions obtained from mathematical simulation can be used for more precise definition of the point source angular coordinates. Also these response functions are suitable for simulation of the angular distribution measurements for several sources with different intensities. Such simulation requires a large set of response functions for different point sources locations. Direct calculations of response functions for entire solid angle are too computationally intensive and can be avoided using detector block symmetry.

Response function is represented by vector of EDR values registered by ShD detectors

$$\mathbf{F}_i = \mathbf{F}_i(\theta_i, \varphi_i) \equiv \begin{pmatrix} H_1^{(i)} \\ \vdots \\ H_{32}^{(i)} \end{pmatrix}. \quad (7)$$

ShD detector block symmetry corresponds to icosahedrons space symmetry group. It means that symmetry transformation of response function for one source direction gives response function for another direction. So it is necessary to obtain icosahedrons symmetry group representation in space of 32-vectors. Thus, set of operators acting on \mathbf{F}_i and representing icosahedrons group is necessary

$$\mathbf{F}'_i = \mathcal{G} \mathbf{F}_i, \quad (8)$$

where \mathcal{G} – operator corresponding to element of the icosahedrons symmetry group. Obviously, \mathcal{G} operator action on vector \mathbf{F}_i gives new vector by permutation of the \mathbf{F}_i elements. Consequently \mathcal{G} operators constitute sub-group of the permutation group [4]. According to the Kelly's theorem, any space symmetry group is isomorphic to some permutation group. Evidently, one-to-one correspondence exists between elements of the crystallographic Y_h icosahedrons symmetry group and \mathcal{G} operators. So problem reduces to construction of \mathcal{G} operators for all elements of the icosahedrons symmetry group.

Below construction of permutation operator for any rotation from symmetry group Y_h . Detector block can be considered as icosahedron with detector collimating apertures located in vertexes and plane centers. Rotation belong to symmetry group Y_h transforms each icosahedron plane into other plane. Thus for construction of permutation operator it is enough to consider transformation of the one fixed icosahedrons plane. Plane containing detector 2 (see Table 2) is the most suitable choice.

To study plane transformation it is necessary to fix its position and orientation. This can be achieved by fixing the plane center and one of its vertices. In our case vertex 1 is an obvious choice. Any rotation from symmetry group can be specified by aperture numbers, which apertures 1 and 2 transform to. Let aperture 1 transform to aperture p , and aperture 2 – to aperture q . Possible values of p and q are shown in Table 2.

Table 2. Plane centers and corresponding vertices

Plane number	Plane center	Vertices
1	2	1, 7, 11
2	3	1, 7, 8
3	4	1, 8, 9
4	5	1, 9, 10
5	6	1, 11, 10
6	12	7, 11, 22
7	13	8, 7, 23
8	14	9, 8, 24
9	15	10, 9, 25
10	16	11, 10, 26
11	17	7, 23, 22
12	18	8, 24, 23
13	19	9, 25, 24
14	20	10, 26, 25
15	21	11, 22, 26
16	27	22, 23, 32
17	28	23, 24, 32
18	29	24, 25, 32
19	30	25, 26, 32
20	31	22, 26, 32

Let \vec{n}_p and \vec{n}_q be unit vectors directed from block geometric center to corresponding apertures. Using these vectors we can construct rotation matrix in

Cartesian space. Let us build mutually orthogonal unit vectors $\vec{e}_x, \vec{e}_y, \vec{e}_z$ that define new coordinate system

$$\begin{aligned}\vec{e}_z &= \frac{\vec{n}_p}{|\vec{n}_p|}, \\ \vec{e}_y &= \frac{\vec{e}_z \times \vec{n}_q}{|\vec{e}_z \times \vec{n}_q|}, \\ \vec{e}_x &= \vec{e}_y \times \vec{e}_z.\end{aligned}\tag{9}$$

Now rotation matrix G is defined by coordinates of vectors \vec{e}_x, \vec{e}_y and \vec{e}_z

$$G = \begin{pmatrix} e_{x1} & e_{y1} & e_{z1} \\ e_{x2} & e_{y2} & e_{z2} \\ e_{x3} & e_{y3} & e_{z3} \end{pmatrix}.\tag{10}$$

Rotation matrix G according to (10) defines transformation of detector coordinates into new coordinate system. Evidently, this matrix is isomorphic to corresponding permutation operator \mathcal{G} .

operator. The goal is to find aperture coordinates after Using rotation matrix G , we can easy obtain explicit form of the permutation rotation n'_i

$$n'_i = G_{ik} n_k,\tag{11}$$

and to determine correspondence between old and new coordinates (Table 1). As the result we obtain 32 permutation rules $\{r \rightarrow r'; r, r' = 1, \dots, 32\}$, where r is aperture number. These rules define permutation operator \mathcal{G} .

2. Mathematical simulation of angle distribution measurements

Mathematical simulation was used for more precise definition of the attenuation coefficients and also for verification of ShD calibration results [5].

According to the formula (6) unfolding of the experimental data requires solution of the linear system. Coefficients α_{ij} depend on the device geometry.

Using GEANT software we have developed mathematical model of ShD detector module and calculated coefficients α_{ij} .

Spherical shape of ShD device stipulates usage of spherical coordinate system. Hence detector coordinates can be written as “latitude” and “longitude”. Direction to the considered detector is defined as $(0^\circ, 0^\circ)$. Direction to the neighboring detector is $(37.4^\circ, 0^\circ)$. Coordinates of all other detector are determined relative to these reference points.

If we look along some aperture axis, we shall see aperture symmetry relative to this axis. Thus we can introduce the term “layer” describing apertures symmetrical relative to the given direction (Fig. 2). All the apertures belong to the same layer have same attenuation coefficients. Thus along the given axis registered EDR can be grouped by layers.

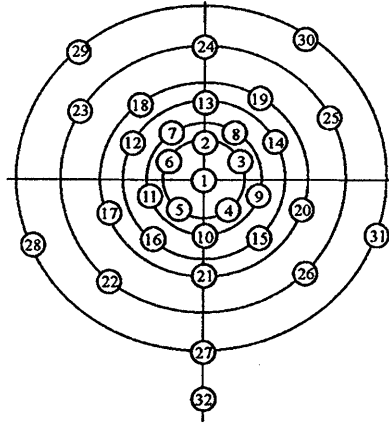


Fig. 2. Detector positions and corresponding layers

Calculation results are given at Fig. 3 and Fig. 4. For the sake of simplicity we have used radiation transmission coefficients instead of attenuation coefficients. Figures show transmission coefficients for detectors in different layers versus distance from radiation source to ShD center. At Fig. 3 radiation source was placed opposite to detector 10 with coordinates $(63.4^\circ; 252^\circ)$ (Table 1), at Fig. 4 radiation source was opposite to detector 5 $(37.4^\circ; 216^\circ)$.

Using mathematical simulation we have obtained ShD response functions for various distances from radiation source. Analysis shows for distances longer than 70 cm transition coefficients and corresponding response functions undergo minor changes. Thus the same response function could be used for all long-distanced radiation sources. Also we have obtained response functions for wide energy range

100 keV...1.5 MeV. These could be used for the enhanced procedure for gamma-radiation spectrum unfolding.

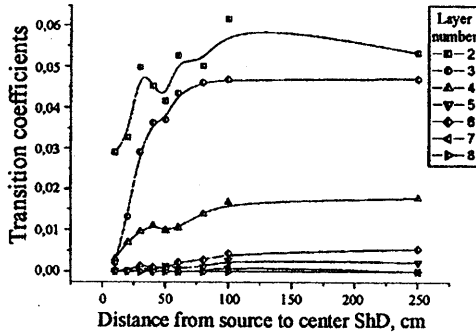


Fig. 3. Transition coefficients for detectors in different layers versus distance “radiation source – ShD center”. Radiation source is opposite to detector 10 with coordinates (63.4°; 252°)

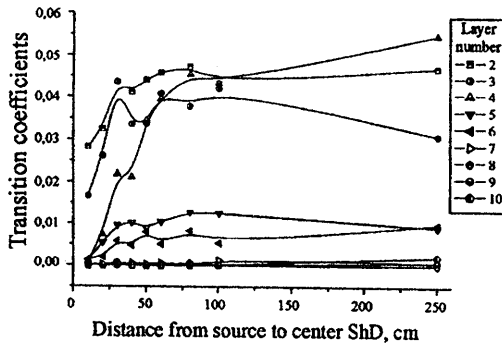


Fig. 4. Transition coefficients for detectors in different layers versus distance “radiation source – ShD center”. Radiation source is opposite to detector 5 with coordinates (37.4°; 216°)

Consistent model for angular gamma-radiation distribution measurement must include ShD detectors response functions. We have developed mathematical model for CdTe detector used in ShD detector module [5-10]. This model considers common physical processes for gamma radiation interaction with detector material. Mathematical simulation using PENELOPE and GEANT-4 codes provided us with

detector energy deposition spectrum. This was the base for detector response function construction.

For simulation we have used cylindrical CdTe detector. Detector was 1 cm diameter and 1 cm thickness. Detector material was CdTe with $6.2 \cdot 10^3 \text{ kg/m}^3$ density [7,8]. PENELOPE was used as basic simulation method for mathematical simulation. In order to speed up calculations and to lower dispersion of the results we used specialized code for systems with cylindrical symmetry.

As detector response function we used deposition spectrum for incident gamma radiation. Calculations considered all possible physical processes for photons: Compton and Relay scattering, photo effect and pair production. We considered large number of the initial events ($2 \cdot 10^6$) to obtain results with small variance. Standard deviation of the obtained results was less then $3.72 \cdot 10^{-9} \text{ 1/(eV}\cdot\text{part)}$.

Deposition spectrum is shown at Fig. 5. We obtained spectra for photon energy range from 50 keV to 1.5 MeV. These spectra were used for procedure of radiation spectrum unfolding. Unfolding procedure bases on the method from work [7]. The main idea of this method is response functions expansion of energy spectrum. Expansion coefficients are amplitudes of initial spectrum for corresponding energies.

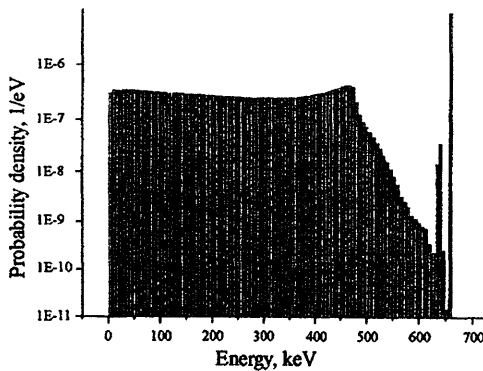


Fig. 5. CdTe-detector energy deposition spectrum CdTe-detector for photon energy 662 keV

During analysis of the angular distribution cartogram it can be difficult to determine the direction to the radiation sources. At the real-world conditions there can be many expanded sources. Problem of source detection has no exact solution. One of the possible approaches is usage of fuzzy-logic methods. In our work we have used neural network method. It is based on the principles of the human brain activity. Development of neural network algorithm requires usage of optimal structure of neural network with effective learning algorithm. Strategy of "learning

with teacher” (Fig. 6) foresees presence of the learning set (X, Y) . Neural network is taught using vectors from the learning set with simultaneous weight correction. Certain procedure is applied until the setup error for all set becomes acceptably low

$$Err = \sum_{i=1}^N |Y_i - Y_i| \rightarrow \min .$$

Dependence of output signal Y versus input signal X can be written in the form $Y = F(W, X) + Err$, where $F(W, X)$ – function from the neural network learning algorithm. In our case it is ShD response for sources. W is parameter set allowing function adjusting for image identification (number of network layers, number of neurons in the layer, matrix of the neural network synaptic weights). Err is error due to imperfect correspondence of the real output signal value to the desired value and also due to calculation errors.

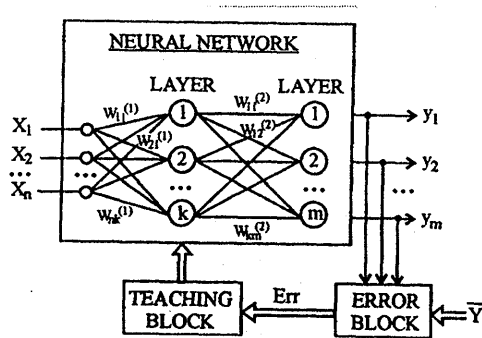


Fig. 6. Multilayer neural network learning algorithm “with teacher”

Now so called error back-propagation algorithm is used for multilayer perceptron learning. Network optimization is aimed on reduction of calculations preserving the necessary solution precision. Parameters of optimization of our network were number of layers number and number of neurons in the hidden layer. Another task was development of good network teaching algorithm allowing network adjustment for identify initial image set at minimal time. Network learning consists in net adjustment so that for certain input it produces desired or close to desired output set.

NeuroData software was developed to obtain the taught set. Its flow block is given at Fig. 7. Software was developed using C++ and produces learning samples with for various input data (number of sources, source location relatively to ShD facility) and corresponding response values.

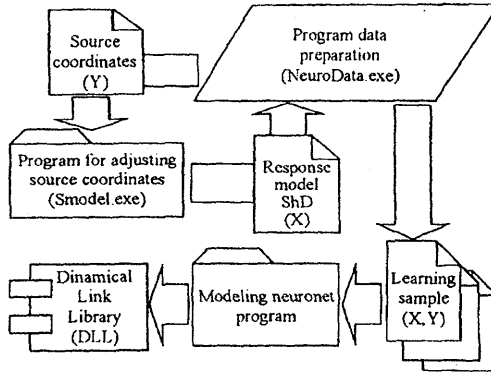


Fig. 7. Neural network learning scheme

Using the measurement results we have optimized number of neurons in the hidden layer (Fig. 8). The optimal neural network has 96 inputs, 3 neurons in hidden layer and 32 outputs (Fig. 9).

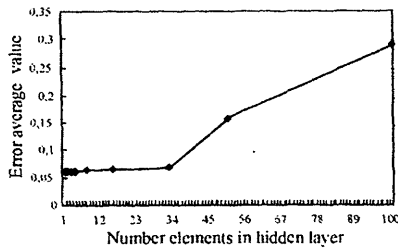


Fig. 8. Neural network error versus number of elements in the hidden layer

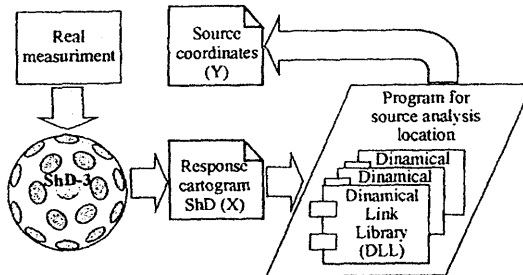


Fig. 9. Scheme of the neuronet models realization usage

Using NeuroData we have formed set of the input and output data. This allowed obtaining corrected source coordinates using measurement data. Set of 1000...2000 simulated source and response values was used for teaching of the networks with different configurations.

Teaching continued until difference between network output and sample input reached minimum. Multilayer perceptron was used as network model. Results neural network teaching for different configurations are given in Table 3. For real measurements using ShD-3 this NeuroData software will allow to obtain the most reliable distribution of the gamma-sources.

Table 3. Results of the neural network simulation

Number of potential sources	Number of existing sources	Number of the elements in the hidden layer	Err, learning error	Number of the learning epochs
1	1	3	0.09	20
3	1	9	0.03	725
5	2	15	0.037	500
10	5	30	0.05	242
20	10	50	0.055	269
32	16	50	0.159	390
32	16	100	0.293	701
32	16	32	0.0656	325
32	16	16	0.0629	998
32	16	8	0.0628	998
32	16	4	0.0622	864
32	16	3	0.0620	634
32	16	2	0.0622	1001
32	16	1	0.0622	104
32	16	3*	0.0622	1001

Rem: *– 2 hidden layers with 3 elements in each.

3. Simulation of point radiation sources for ShD device

Simulation of point gamma-radiation sources was performed using the algorithm from section 1 and response functions for the plane 1 from mathematical simulation.

By definition response functions describe EDR values registered by ShD detectors for point source. From the section 1 it follows using ShD symmetry transformation one can obtain response functions for other source locations. This result can be used for simulation of measurements procedure with several point sources. Corresponding response functions were obtained from the initial response function set using the symmetry transformation (7). Resulting response function is the sum of response functions for all sources. Normalizing the response functions and introducing the weight coefficients defining relative intensities, one can simulate set of sources with different intensities. If response functions are normalized to unity, then multiplication of the simulation results by source intensity gives detector values in terms of the exposure dose rate.

Simulation of multiple sources uses the following algorithm, which is applied to each source. Source angular coordinates and weight coefficients are the input data.

Step 1: transformation from the angular coordinates of the source, detectors (Table 1) and model sources to Cartesian coordinates on the unit sphere.

Step 2: selection of the nearest to the source detector among the plane-centered detectors (Table 4).

Step 3: selection of the nearest to the source vertex detector belonging to the plane chosen at step 2.

Step 4: calculation of vectors \vec{n}_0 and \vec{n}_z from the detector coordinates (step 2 and 3).

Step 5: calculation of vectors \vec{e}_x , \vec{e}_y , \vec{e}_z and rotation matrix R using relations (8) and (9).

Step 6: transformation of source coordinates using rotation matrix R to plane 1 (Table 3.1) and nearest model source is selection.

Step 7: transformation of model source coordinates using inverse matrix R^{-1} .

Step 8: multiplication of detector values by source intensity and are addition to result.

Repeating this procedure for all sources we obtain the resulting response function. It describes EDR values registered by ShD detectors (in relative units) for set of sources with given coordinates and relative intensities.

This algorithm was implemented in the computing program using FORTRAN 90. Input data is given in the text file with sources coordinates and relative intensities.

Table 4. Plane centers and corresponding plane vertices

Plane number	Plane center number	Plane vertices numbers	Plane number	Plane center number	Plane vertices numbers
1	2	1, 7, 11	11	17	7, 23, 22
2	3	1, 7, 8	12	18	8, 24, 23
3	4	1, 8, 9	13	19	9, 25, 24
4	5	1, 9, 10	14	20	10, 26, 25
5	6	1, 11, 10	15	21	11, 22, 26
6	12	7, 11, 22	16	27	22, 26, 32
7	13	8, 7, 23	17	28	23, 22, 32
8	14	9, 8, 24	18	29	24, 23, 32
9	15	10, 9, 25	19	30	25, 24, 32
10	16	11, 10, 26	20	31	26, 25, 32

Developed software was used for simulation of the ShD measurements in the case of the several sources and also for estimation of ShD angular resolution. Comparison of simulation results with calibrating measurements results shows that developed method adequately describes ShD parameters and can be used for simulation of measurements in case of several sources with different intensities.

To estimate ShD angular resolution we simulated the radiation of the two sources with equal intensities. Direction to the first source was constant: $\varphi = 0$, $\theta = 79.2$. Direction to the second source changed with step 1° in the upper hemisphere $\varphi = 0$, $\theta = 0 \dots 79.2$. Simulation results for angles $\theta_2 = 0^\circ, 12^\circ, 53^\circ$ and 62° are shown at Fig. 10, a – d.

At the Fig. 10, a radiation from the two sources is registered by detectors 1 and 16 (detector numbers – see Table 1). At Fig. 10, b and Fig. 10, c radiation is registered by detectors 1, 6 and 16. At Fig. 10, d – two sources are unresolved and radiation is registered by detector 16. Thus, simulation results showed that for θ_2 above 62° two sources are not resolved. So ShD angular resolution is approximately

$79.2^\circ - 62^\circ = 17.2^\circ$. Taking into account calculation errors, we obtain ShD angular resolution approximately 15° .

So, the developed method can be used for more precise calibration of the ShD device, detector block angular distribution estimation and for the development of the certification procedure for the ShD device.

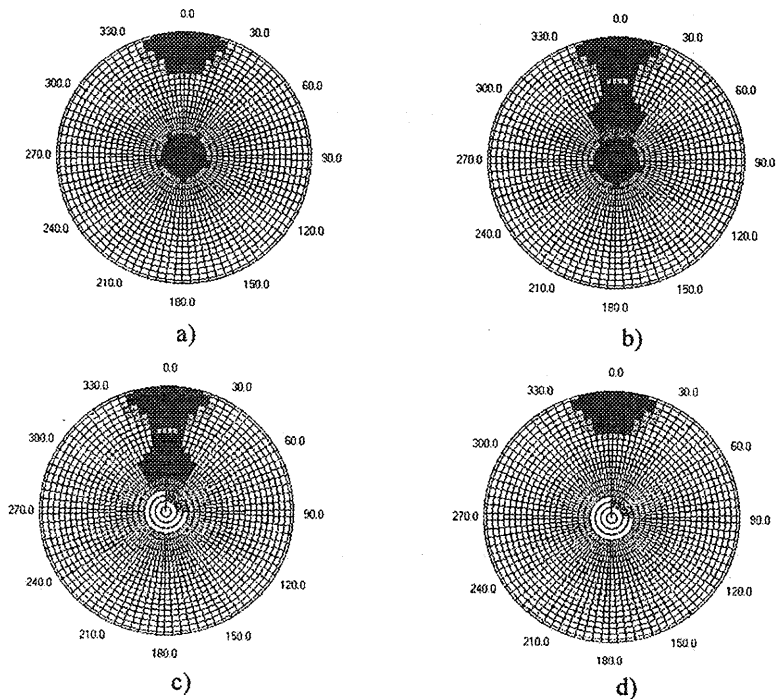


Fig. 10. Simulation results for the radiation of the two sources placed at: 0° i $79,2^\circ$ (a); 12° i $79,2^\circ$ (b); 53° i $79,2^\circ$ (c); 62° i $79,2^\circ$ (d)

4. Mathematical simulation of "Shelter object" gamma-radiation spectrum

For mathematical modeling we have used MCNPX software that implements Monte-Carlo method. All possible physical processes for photon interaction, i.e., coherent scattering, photoeffect with luminescence, Compton effect and pair production were considered.

For simulation purposes we have calculated spectra in the barrier geometry for different concrete and lead layers. Gamma-quanta spectral distribution is shown at Fig. 11. It was supposed that open sources are absent and gamma-radiation spectrum is formed mainly by radiation passing through the concrete constructions. Estimations showed contribution from air-scattered radiation ("Sky shine" effect) to doze doesn't exceed several percents. So gamma-radiation spectrum was simulated by radiation with initial photon energy 661.1 keV passed through the concrete

layer (from 20 to 60 cm thickness). Visualization of the concrete+cesium volume source is presented in Fig. 12. Results are given at Fig. 13 and Fig. 14.

Average gamma-radiation energy is 300...380 keV behind the concrete. It is slightly lower than experimentally obtained effective energy value (350...400 keV). Spectra (Fig. 13 and Fig. 14) and average energy (Fig. 15) vary slightly for concrete thicknesses from 20 to 60 cm. It can explain the experimental fact that gamma-radiation effective energy is nearly the same for different places at the "Shelter" object and near it.

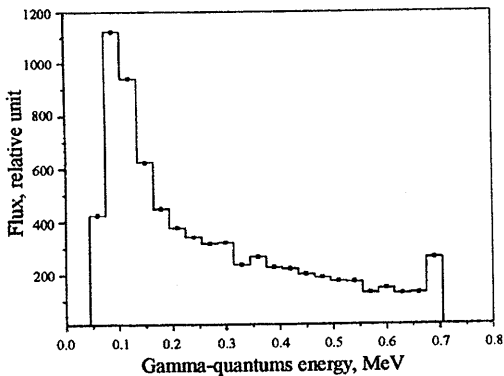


Fig. 11. Gamma-radiation spectrum

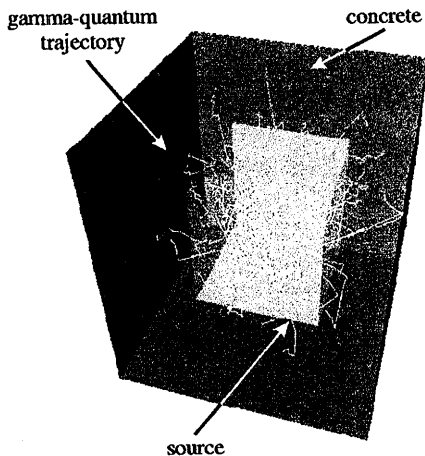


Fig. 12. Visualization of the concrete volume source

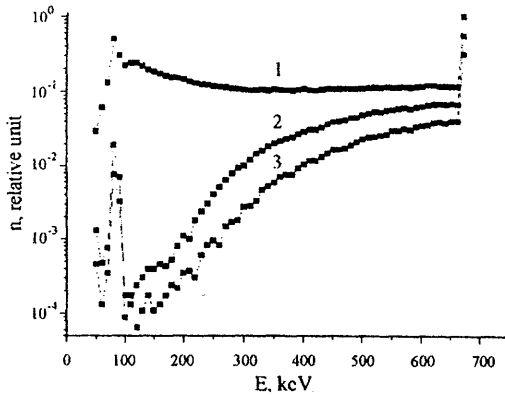


Fig. 13. ^{137}Cs spectra after concrete and lead layers: 1 – concrete 30 cm; 2 – concrete 30 cm + lead 0.5 cm; 3 – concrete 30 cm + lead 1.0 cm

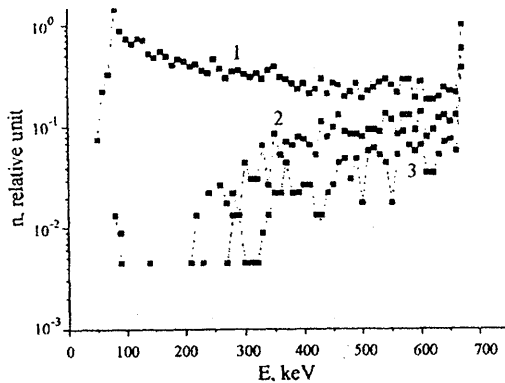


Fig. 14. ^{137}Cs spectra after concrete and lead layers: 1 – concrete 60 cm; 2 – concrete 60 cm + lead 0,5 cm; 3 – concrete 60 cm + lead 1,0 cm

After the lead shield spectrum average energy increases up to 530...580 keV depending on the concrete and lead thickness. This value is also slightly lower than experimentally measured gamma-radiation effective energy (550...600 keV).

Gamma-radiation spectra measurements can be useful to examine the presence of the open or badly shielded sources, to reveal large contribution from the scattered radiation, to verify experimental methods and mathematical results.

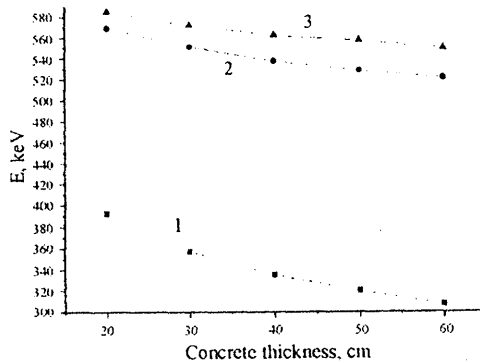


Fig. 15. Gamma-radiation average energy after concrete layers: 1 – concrete; 2 – concrete + lead 0.5 cm; 3 – concrete + lead 1.0 cm

Results of gamma-spectra modeling will be used for estimation of the efficiency of the gamma-radiation registration during planning of the measurements near the "Shelter" object and also for the control of the radioactive waste packages transportation during the "Shelter" object transformation to the ecological safe system. These data will also be used for the development of the technical requirements for the used detectors.

CONCLUSIONS AND DISCUSSIONS

Mathematical model of detector block was developed and response function for the gamma-radiation angular distribution measurement was calculated. These data are the necessary initial data for measurements with ShD device, that is being created, and for further processing of the data obtained during the measurements.

The "Shelter" objects gamma-radiation spectrum was simulated. Such data are necessary to develop the technical requirements for the detectors of the ShD-3 facility and to determine boundary conditions and to optimize measurement method.

Special software was developed for experimental data processing and angular distribution unfolding. This software was used to simulate experiments with ShD facility in the case of several sources and to estimate ShD angular resolution.

Neural network method for detection of the direction to the several sources was developed. It can be used for in situ measurements with many not point sources. Such tasks are effectively solved using fuzzy logic methods. Practical measurements using ShD-3 device software based on the neural network algorithm will give the most reliable gamma-sources distribution.

This work was supported by STCU project 3511.

REFERENCES

1. В.Г. Батий, В.В. Егоров, Н.А. Кочнев и др. Методика оценки угловых распределений мощности дозы гамма-излучения в зонах производства работ на объекте “Укрытие” // *Проблеми Чорнобиля. Науково-технічний збірник*. Чорнобиль: 2002, вип. 9, с. 47-52.
2. V. Batiy, O. Pravdiviy, O. Stoyanov et al. *A Practical Method for Measuring Angular Distribution of Radiation from Multiple Gamma Sources*. Proceedings of “2007 Waste Management Symposium Global Accomplishments in Environmental and Radioactive Waste Management: Education and Opportunity for the Next Generation of Waste Management Professionals”. CD, 2007, # 7160.
3. Дж. Элиот, П. Добер. *Симметрия в физике*. Т. 2. М.: Мир, 1983, 410 с.
4. В.Г. Батий, В.В. Егоров, А.И. Стоянов, С.И. Прохорец, Е.В. Рудычев, Д.В. Федорченко, М.А. Хажмурадов и др. Математическое моделирование углового разрешения многодетекторной установки для поиска интенсивных источников гамма-излучения // *Сборник научных трудов СНИЯЭиП*. Севастополь, 2007, №3(23), с. 15-21.
5. В.Г. Батий, В.М. Рудько, И.М. Прохорец, М.А. Хажмурадов и др. Методика измерений угловых распределений гамма-излучения с применением полупроводниковых детекторов // *Сборник научных трудов СНИЯЭиП*. Севастополь, 2007, №4(24), с. 13-20.
6. G.H. Yoo, K.J. Chun, S.H. Ha. *Unfolding of the Measured Spectra and Determination of Correction Factors of a Free Air Ionization Chamber using EGS4 Simulation Proceedings of the Second International Workshop on EGS*. 8-12 August 2000, Tsukuba, Japan KEK Proceedings 200-20, p. 308-315.
7. А.А. Захарченко, В.Е. Кутний, И.М. Прохорец, М.А. Хажмурадов. Моделирование влияния шумов на характеристики CdZnTe -детекторов γ -излучения // *Радиоэлектроника и информатика*. 2007, №1(36), с. 13-16.
8. А.А. Захарченко, А.В. Рыбка, В.Е. Кутний, М.А. Хажмурадов и др. Моделирование энергетической зависимости чувствительности CdTe (CdZnTe) -детекторов гамма-излучения // *Технология и конструирование в электронной аппаратуре*. 2007, №1, с. 28-31.
9. А.А. Захарченко, В.Е. Кутний, И.М. Прохорец, М.А. Хажмурадов. Определение параметров переноса заряда в CdTe-детекторах γ -излучения методами математического моделирования // *Радиоэлектроника. Информатика. Управління*. 2007, №2(18), с. 13-15.
10. А.А. Захарченко, В.Е. Кутний, И.М. Прохорец, М.А. Хажмурадов. Методы определения параметров переноса заряда в CdTe (CdZnTe)-детекторах гамма-излучения // *Вісник Харківського університету. Серія: Ядра, частинки, поля*. 2007, вип. 4(36), с. 85-92.

Валерий Григорьевич Батий, Евгений Валерьевич Батий, Владимир Владимирович Егоров, Дмитрий Владимирович Федорченко, Ольга Анатольевна Кафтанатина, Манап Ахмадович Хажмурадов, Николай Александрович Кочнев, Виктория Владимировна Селюкова, Александр Иванович Стоянов, Светлана Ивановна Прохорец, Иван Михайлович Прохорец, Егор Владимирович Рудычев, Валентина Петровна Лукьянова

**МАТЕМАТИЧЕСКОЕ МОДЕЛИРОВАНИЕ ПРОЦЕССА ИЗМЕРЕНИЯ
УГЛОВЫХ РАСПРЕДЕЛЕНИЙ ГАММА-ИЗЛУЧЕНИЯ**

Ответственный за выпуск Л.М. Ракивненко

Редактор, корректор Т.И.Бережная
Компьютерный макет Т.И. Бережная

Подписано в печать 15.04.08. Формат 60x84/16. Ризопечать. Усл.п.л. 1,4.
Уч.-изд.л 0,9. Тираж 100 экз. Заказ №29.

Национальный научный центр «Харьковский физико-технический институт»
61108, г.Харьков, ул.Академическая, 1

